Thermoresponsive Transport through Porous Membranes with Grafted PNIPAM Gates

Liang-Yin Chu, Takuya Niitsuma, Takeo Yamaguchi, and Shin-ichi Nakao
Dep. of Chemical System Engineering, The University of Tokyo, Tokyo 113-8656, Japan

Both thermoresponsive flat membranes and core-shell microcapsule membranes, with a porous membrane substrate and grafted poly(N-isopropylacrylamide) (PNIPAM) gates, were successfully prepared using a plasma-graft pore-filling polymerization method. PNIPAM was proven to be grafted homogeneously onto the porous membrane substrates, in the direction of both the membrane thickness and surface. Regardless of the solute molecular size, temperature had an opposite effect on diffusion coefficients of the solute across the PNIPAM-grafted membranes with low graft yields as opposed to those with high graft yields. The PE-g-PNIPAM membranes change from positive thermo-response to negative thermoresponse types with increasing pore-filling ratios at around 30%. Phenomenological models were developed for predicting the diffusion coefficient of the solute across PNIPAM-grafted membranes at temperatures, both above and below the lower critical solution temperature (LCST). Predicted diffusional coefficients of solutes across both the PNIPAM-grafted flat and PNIPAM-grafted microcapsule membranes fit the experimental values. To obtain an ideal result for the diffusional thermoresponsive controlled release through PNIPAM-grafted membranes, the substrates strong enough to prevent any conformation changes are more suitable for preparing thermoresponsive membranes than weak ones.

Introduction

Environmental stimuli-responsive gating membranes, which are composed of porous membrane substrates and stimuli−responsive functional gates, have been widely investigated in recent years. The hydraulic permeability (pressure-driven convective flow of solvents) and the diffusional permeability (concentration-driven molecular diffusion of solutes) of these membranes can be controlled or adjusted by the gates according to the external chemical and/or physical environment. Serving as chemical valves, these gates have been reported to act in response to changes in environmental temperature (Okahata et al., 1983, 1986; Iwata et al., 1991; Kubota et al., 1994; Chen et al., 1997; Peng and Cheng, 1998; Choi et al., 2000a,b; Chu et al., 2001a,b, 2002a), pH (Osada et al., 1986; Okahata et al., 1987; Iwata and Matsuda, 1988; Ito et al., 1990, 1992, 1997b,c; Islam et al., 1992; Israels et al., 1994; Lee et al., 1995; Lee and Shim, 1996; Ulbricht, 1996; Hautojarvi et al., 1996; Shim et al., 1999; Peng and Cheng, 2000), ionic strength (Osada et al., 1986; Iwata and Matsuda, 1988; Kim and Anderson, 1989; Islam et al., 1992; Ito et al., 1992; Mika et al., 1995; Hautojarvi et al., 1996), glucose concentration (Ito et al., 1989; Cartier et al., 1995), external electric field (Bhaskar et al., 1985; Ly and Cheng, 1993), photo irradiation (Chung et al., 1994), oxidoreduction (Ito et al., 1997a), or substance species (Yamaguchi et al., 1999; Chu et al., 2002b). As there are many cases in which environmental temperature fluctuations occur naturally, and in which the environmental temperature stimuli can be easily designed and artificially controlled, much attention has recently focused on thermoresponsive membrane systems (Iwata et al., 1991; Kubota et al., 1994; Chen et al., 1997; Peng and Cheng, 1998; Choi et al., 2000a, 2000b; Chu et al., 2001a,b; 2002a).

One of the main methods to prepare the just-mentioned membranes is by grafting stimuli−responsive functional polymers onto porous membrane substrates using various techniques (Okahata et al., 1986, 1987; Osada et al., 1986; Iwata and Matsuda, 1988; Ito et al., 1989, 1990, 1992, 1997a,b,c; Iwata et al., 1991; Kubota et al., 1994; Islam et al., 1992; Chung et al., 1994; Israels et al., 1994; Cartier et al., 1995;

Correspondence concerning this article should be addressed to T. Yamaguchi.
Current address of L.-Y. Chu: School of Chemical Engineering, Sichuan University, Chengolu, Sichuan 610065, China.

Lee et al., 1995; Lee and Shim, 1996; Ulbricht, 1996; Hautojarvi et al., 1996; Chen et al., 1997; Peng and Cheng, 1998; Shim et al., 1999; Yamaguchi et al., 1999; Choi et al., 2000a,b; Peng and Cheng, 2000; Chu et al., 2001a,b, 2002a,b). As the grafted polymeric chains should have freely mobile ends, which are different from the typical cross-linked network structure of the hydrogels that gives rise to relatively immobile chain ends, the responsiveness of the prepared membranes to the environmental stimuli could, therefore, be faster than that of their corresponding homogeneous analogs, owing to the more rapid conformational changes of the functional polymers (Yoshida et al., 1995; Peng and Cheng, 1998; Yamaguchi et al., 1999). The grafted polymers can be located either mainly on the external membrane surface, or on both the external surface and the inside of the pores, depending on the grafting conditions. However, globally grafted membranes are expected to exhibit a more pronounced response than those with primarily surface grafts (Kubota et al., 1994; Peng and Cheng, 1998).

Recently, both thermoresponsive flat membranes and core-shell microcapsule membranes, with a porous membrane substrate and poly(*N*-isopropylacrylamide) (PNIPAM) chains grafted onto the pore surfaces throughout the entire membrane thickness, have been prepared (Peng and Cheng, 1998; Choi et al., 2000a,b; Chu et al., 2001a,b, 2002a). For both the thermoresponsive flat membranes and the microcapsule membranes, an interesting result has been reported, in that temperature has an opposite effect on the solute diffusion coefficients of the membranes with low graft yields as opposed to those with high graft yields. This indicates that two distinct types of gating functions exist as a positive thermoresponse type and negative thermoresponse type, depending on the graft yield (Peng and Cheng, 1998; Chu et al., 2001a,b). Besides the effect of the graft yield, the effect of the molecular size of the solutes on the diffusion coefficient was also investigated in these studies (Peng and Cheng, 1998; Chu et al., 2001a,b, 2002a). However, an understanding of the morphological control of the porous membranes with linear-grafted PNIPAM gates, of the effect of membrane morphology on the thermoresponsive transport behavior, and of the prediction of the thermoresponsive transport behavior with morphological parameters, is still lacking.

In this study, both thermoresponsive flat membranes and core-shell microcapsule membranes, with a porous membrane substrate and grafted PNIPAM gates, were prepared using a plasma-graft pore-filling polymerization method (Yamaguchi et al., 1991, 1996, 1999; Choi et al., 2000a,b; Chu et al., 2001a,b, 2002a,b). Investigations were carried out on the morphological control of the porous membranes with linear-grafted PNIPAM gates, on the effect of membrane morphology on the thermoresponsive solute diffusion coefficient, and on the estimation of the thermoresponsive diffusional transport behavior with morphological parameters, in order to obtain some guidance for the design of this type of thermoresponsive membranes.

Phenomenological Models

Until now, phenomenological models seldom have been reported for describing the diffusion behavior of solute across grafted porous membranes. Especially, no phenomenological models have been developed for predicting the thermoresponsive solute diffusion coefficient of PNIPAM-grafted porous membranes. Owing to a phase transition of the grafted PNIPAM gates in the pores of the membranes, the physical condition of the PNIPAM-grafted membranes at temperatures above the lower critical solution temperature (LCST) of PNIPAM is different from that below the LCST. Therefore, different models need to be developed for describing the diffusion phenomena of solute across PNIPAM-grafted membranes at temperatures above and below the LCST, respectively.

Diffusion model above the LCST

Above the LCST, the PNIPAM gates in the membrane pores are in the hydrophobic and shrunken state; the solute can move through the membrane only if it finds a pore with a diameter greater than the diameter of the solute. The diffusion coefficient of the solute is dependent on the sieving behavior of the membrane.

The sieving factor of the membrane can be described as

$$P(r_s) = \int_{x_o}^{\infty} f(x)\,dx \tag{1}$$

where $P(r_s)$ is the probability of a solute with a radius, r_s, moving into a given pore in the membrane, $f(x)$ is the differential distribution function of the pore diameter, x is the diameter of the pore, and x_o is the critical pore diameter required to allow solute entrée.

Therefore, the diffusion coefficient of solute across the membrane at temperatures above the LCST will be

$$D_m = P(r_s) \cdot k_m \cdot D_o \tag{2}$$

where D_m is the diffusion coefficient of solute across the membrane, k_m is an obstruction constant reflecting both the porosity and the pore tortuosity for a given membrane substrate (ungrafted), and D_o is the diffusion coefficient at infinite dilution calculated following the Stokes–Einstein equation, denoted by

$$D_o = \frac{k_B T}{6\pi\mu r_s} \tag{3}$$

where k_B is Boltzmann's constant, T is the absolute temperature, μ is the viscosity of solvent, and r_s is the Stokes–Einstein radius of the solute.

Although a number of researchers have also used expressions for $P(r)$ for describing the obstruction effect or sieving effect in solute diffusion (Ogston, 1958; Yasuda et al., 1969; Johansson et al., 1991; Amsden, 1998b, 1999), they were describing solute movement within a hydrogel. Here the commonly used Weibull second-order distribution (shape parameter $m = 2$, and position parameter $\gamma = 0$) is introduced to describe the pore size distribution, and the probability den-

sity function is given by

$$\begin{cases} f(d_x) = \dfrac{2}{\alpha} d_x \cdot \exp\left(- \dfrac{d_x^2}{\alpha} \right) \\ d_g = \alpha^{(1/2)} \Gamma\left(\dfrac{3}{2} \right) \end{cases} \tag{4}$$

that is,

$$f(d_x) = \frac{2[\Gamma(1.5)]^2}{d_g^2} d_x \exp\left\{ -[\Gamma(1.5)]^2 \left(\frac{d_x}{d_g} \right)^2 \right\}$$

$$= 1.5707 \frac{d_x}{d_g^2} \exp\left[-0.7854 \left(\frac{d_x}{d_g} \right)^2 \right] \tag{5}$$

where d_x is the pore diameter, and d_g is the mean value of the pore diameters of the grafted membranes. Let $x_o = 2r_s$, then Eq. 1 becomes

$$P(r_s) = \exp\left[-3.1416 \left(\frac{r_s}{d_g} \right)^2 \right] \tag{6}$$

Therefore, the diffusion coefficient of the solute across the membrane above the LCST is given by

$$D_m = \exp\left[-3.1416 \left(\frac{r_s}{d_g} \right)^2 \right] \cdot k_m \cdot \frac{k_B T}{6\pi\mu r_s} \tag{7}$$

in which the obstruction constant k_m for a given membrane substrate (ungrafted) can be calculated by

$$k_m = \exp\left[3.1416 \left(\frac{r_s}{d_o} \right)^2 \right] \cdot \frac{6\pi\mu r_s (D_m)_o}{k_B T} \tag{8}$$

where d_o is the mean value of the pore diameters of the ungrafted membrane substrate, and $(D_m)_o$ is the diffusion coefficient of solute across the ungrafted membrane substrate.

That is, above the LCST, the diffusion coefficient of a solute with radius r_s across the membrane can be predicted by knowing the characteristics of the membrane substrate before grafting and the pore-size distribution of the PNIPAM-grafted membrane.

Diffusion model below the LCST

Below the LCST, the PNIPAM gates in the membrane are in the hydrophilic and swollen state, that is, the gates are in the hydrogel state. The diffusion behavior of the solute is then of one that is able to pass through a hydrogel. The solute transport within the hydrogels occurs primarily within the water-filled regions in the space delineated by the polymer chains (Amsden, 1998a). The diffusion coefficient of the solute can be described using the following equation, which is derived from hydrodynamic theory (Cukier, 1984; Amsden, 1998a)

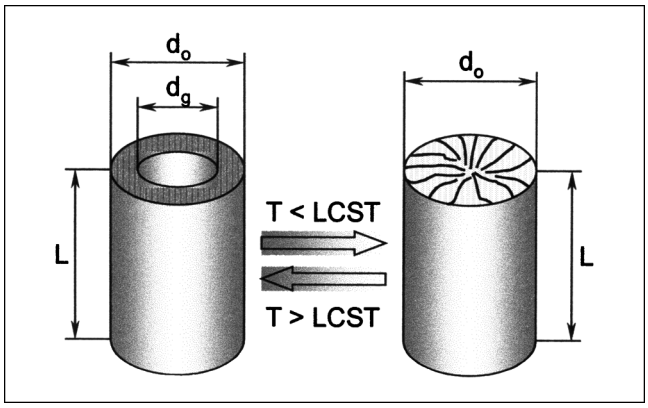

Figure 1. Conformational change of a PNIPAM-grafted pore of a membrane.

$$D_g = \exp\left(- k_c r_s \varphi^{0.75} \right) \cdot k_m \cdot D_o \tag{9}$$

where D_g is the diffusion coefficient in the hydrogel, k_c is a constant for a given polymer–solvent system, and φ is the volume fraction of the polymer in the gel.

As can be seen from the experimental data in the following sections, using plasma-graft pore-filling polymerization, PNIPAM can be homogeneously grafted onto the inner pore surfaces of the porous membrane substrates. Therefore, the volume fraction of polymer in the gel can be determined by measuring the pore diameters at temperatures above the LCST, before and after grafting the PNIPAM chains, as shown in Figure 1. In Figure 1, d_o is the pore diameter before grafting the PNIPAM gates, d_g is the pore diameter after the grafting, and L is the pore length. Then, the volume fraction of polymer in the gel is

$$\varphi = 1 - \left(\frac{d_g}{d_o} \right)^2 \tag{10}$$

Therefore, below the LCST, the diffusion coefficient of a solute across the PNIPAM-grafted membrane can be predicted by detecting the pore-filling ratio of the membrane at temperatures above the LCST.

Experimental Studies

Materials

Porous polyethylene (PE H2100) film was used as the flat porous membrane substrate. The PE H2100 substrate, with a thickness of 100 μm, a porosity of 69%, and a pore size of 0.28 μm, was supplied by Asahi Chemical Co. Ltd., Japan. Terephthaloyl dichloride (TDC) was purchased from Tokyo Kasei Kogyo Co., Ltd., Japan. Ethylene diamine (EDA), sodium dodecyl sulfate (SDS), benzene, xylene, sodium carbonate, sodium chloride (NaCl, molecular weight = 58), carbazochrome sodium sulfonate (CCSS; molecular weight = 322), phosphate pH standard equimolal solution (pH = 6.86),

and vitamin B_{12} (VB_{12}; molecular weight = 1,355) were all purchased from Wako Pure Chemical Industries, Ltd., Japan, and myoglobin (MYO; molecular weight = 18,800) was purchased from Sigma Chemical Co., USA. The solvents used were all of reagent grade. All these chemicals were used as received, and without any further purification. The *N*-isopropylacrylamide (NIPAM) was kindly provided by Kohjin Co., Ltd., Japan, and was used after purifying by recrystallization in hexane and acetone, and then dried *in vacuo* at room temperature.

Preparation of the core-shell microcapsules with a porous membrane

The microcapsules with polyamide porous membranes were prepared using the interfacial polymerization method as described in an earlier publication (Chu et al., 2001a). The molecular formula of the interfacial polymerization reaction is illustrated in Figure 2. First, 10 mL of the organic solvent mixture of benzene/xylene (2:1 [v/v]) containing 0.5 mol/L TDC, was added to 160 mL of the water phase containing 1.0 wt. % SDS as an emulsifier. Then, the mixture was mechanically agitated for 10 min with a stirring speed of 800 rpm to yield an oil-in-water emulsion. The stirring speed was then reduced to 200 rpm, and both the buffer (20 mL water containing 1.18 mol/L sodium carbonate) and 15 mL of monomer EDA were added to the emulsion, and the mixture stirred for a further 5 min. During emulsification and interfacial polymerization, the temperature was kept at a constant 10°C using a thermostatic unit (COOLNIT CL-80F, TAITEC, Japan). The microcapsules were separated by centrifugation, and washed three times using deionized water to remove any emulsifier and remnants of the monomer. These were then dialyzed against deionized water, and freeze-dried.

Grafting the linear PNIPAM chains into the pores of both the flat membranes and the microcapsule membranes by plasma-graft pore-filling polymerization

Plasma-graft pore-filling polymerization was employed to graft the linear PNIPAM chains into either the pores of the flat membrane or the microcapsule membranes according to the method described previously (Yamaguchi et al., 1991, 1996, 1999; Choi et al., 2000a,b; Chu et al., 2001a,b, 2002a,b). Briefly, the flat membrane or the freeze-dried microcapsules were placed in a transparent glass tube, which was then filled with argon gas. The tube was then evacuated to a pressure of 10 Pa, and the flat membrane or microcapsules were subjected to a radio-frequency plasma operating at 13.56 MHz, delivering 30 W for 60 s. Then, under inert atmospheric conditions, the flat membrane or microcapsules were immersed into the NIPAM monomer solution, and the graft polymerization was carried out under vibration in a constant-temperature bath (30°C) for a fixed period. The experimental parameters of the plasma-graft pore-filling polymerization are shown in Table 1. The PNIPAM-grafted microcapsules were separated centrifugally and washed three times with deionized water, and then dialyzed against deionized water and freeze-dried. The PNIPAM-grafted flat membrane was washed three times with a 50% aqueous ethanol solution, and then rinsed in a 50% aqueous ethanol solution under vibration in a constant-temperature bath (30°C) for 24 h to remove any nonreacted monomer and homopolymer. It was then dried in a vacuum oven at 50°C. The quantitative measure of grafting onto the flat membrane was defined as the weight of the grafted polymer per square centimeter of the substrate film.

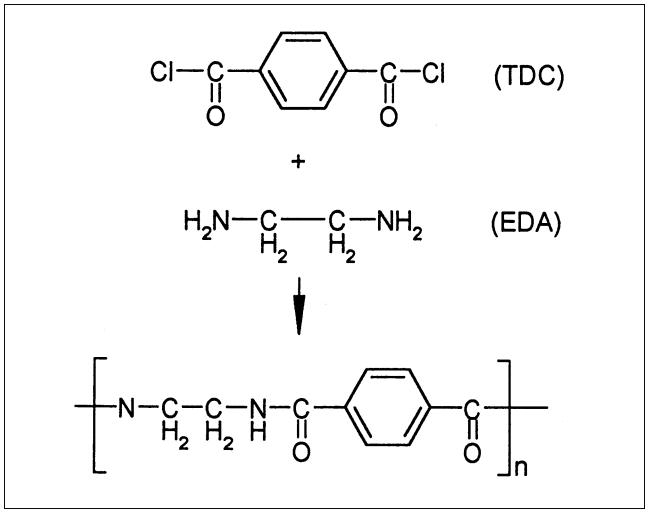

Figure 2. Molecular formula of the interfacial polymerization reaction for preparing porous polyamide microcapsule membranes.

Morphological analysis

The grafted polymer formation profile of the flat porous substrate was measured using the microscopic Fourier transform infrared (FT-IR) mapping method (MAGNA-IR 560 with Nic-Plan, Nicolet, USA). The PE-g-PNIPAM membrane sample was sliced using a microtome, and the sliced sample was scanned by FT-IR. The spectra were collected in up to 10-μm steps along the membrane axial thickness. The aperture size of each measurement was 10×50 μm^2. The profile of the grafted polymer formation was obtained by measuring the ratio of the characteristic PNIPAM peak (amide II peak, 1,550 cm^{-1}) to the characteristic polyethylene substrate peak (methylene peak, 1,450 cm^{-1}).

Table 1. Plasma-Graft Polymerization Parameters for Grafting NIPAM into Pores of the Flat and Microcapsule Membranes

Parameters	PE Flat Membranes	Microcapsules
Monomer solution		
NIPAM concentration	1 wt. %, 5 wt. %	1 wt. %
Water	40 mL	40 mL
Plasma treatment		
Plasma power	30 W	30 W
Treatment time	60 s	60 s
Atmosphere	Ar	Ar
Pressure	10 Pa	10 Pa
Graft polymerization		
Grafting temperature	30°C	30°C
Grafting time	56–1,282 min	20–120 min

Because the membrane thickness of the prepared microcapsule was too small (about 2 μm) to be analyzed by the FT-IR mapping method, a field emission scanning electron microscope (FE-SEM S-900S, Hitachi, Japan) was used to observe the freeze-dried ungrafted and PNIPAM-grafted microcapsules. The cross-sectional structures of the microcapsules were observed by cutting the microcapsules with a microtome knife.

The pore sizes of the PNIPAM-grafted PE membranes at temperatures above the LCST of PNIPAM were measured by the mercury intrusion method (Autopore II 9220, Shimadzu Techno Research, Japan). The pore condition of the PNIPAM-grafted PE membranes at temperatures below the LCST of PNIPAM was determined by the bubble-point method (Perm-Porometer, Seika Co., Japan). The fluid used in the measurements was water, and the temperature was 28–29 °C.

The pore-size distribution of the freeze-dried microcapsule membranes, both before and after grafting the PNIPAM chains into the pores, was determined by the Brunauer–Emmett–Teller (BET) nitrogen adsorption method (ASAP-2010, Micromeritics, USA).

The distribution of the diameters of the emulsions and microcapsules was determined using a Coulter Multisizer (Coulter Counter Multisizer II, Coulter Corporation, USA). A dispersion of the microcapsules was diluted with a balanced electrolyte solution (ISOTON II-pc, Beckman Coulter, Inc., USA). The total surface area and the total volume of the microcapsules in one unit volume of microcapsule dispersion were calculated from the size distribution.

Thermoresponsive diffusion experiments

The solute diffusion efficient experiments of the flat membranes were carried out using a standard side-by-side diffusion cell. The diffusion cell was located in a constant-temperature incubator (EYELA LTI-601SD, Tokyo Rikakikai Co., Ltd., Japan) to keep the diffusional temperature constant. Each test membrane was immersed in the permeant solution overnight before starting the diffusion experiments. The solutes used were NaCl, CCSS, and VB_{12}. Deionized water was used as the liquid in the receptor cell. The concentration of NaCl was determined by measuring the electrical conductance with an electrical conductivity meter (TOA EC Meter 50AT, TOA Electronics Ltd., Japan). The concentrations of CCSS and VB_{12} were determined using a UV–visible recording spectrophotometer (U-3310, Hitachi, Japan) at wavelengths of $\lambda = 363$ nm and 361 nm, respectively.

The diffusion coefficient of solute across the flat membrane, D, can be calculated using the following equation, derived from Fick's first law of diffusion

$$D = \frac{V_1 V_2}{V_1 + V_2} \cdot \frac{L}{A} \cdot \frac{1}{t} \cdot \ln \frac{(C_1)_0}{(C_1)_t - (C_2)_t} \tag{11}$$

where $(C_1)_0$ and $(C_1)t$ are the initial and intermediary concentrations (at time t) of the solute in the donor compartment, respectively; $(C_2)_t$ is the intermediary concentration (at time t) of the solute in the receptor cell; V_1 and V_2 are the volumes of the liquids in the donor compartment and in the receptor compartment, respectively; L is the thickness of the dry membrane; and A is the effective diffusion area of the membrane.

The microcapsule thermoresponsive diffusional experiments were carried out using a previously published method (Chu et al., 2001a). Briefly, the diffusion coefficient of the solute across the microcapsule membranes was measured by determining the increase in the solute concentration of the surrounding medium with time, after mixing a known volume of microcapsule dispersion with a known solute concentration, with the same volume of deionized water (for myoglobin, a buffer solution was used instead of the deionized water). During the measurements, the liquid's temperature was kept constant using a thermostatic unit (COOLNIT CL-80F, TAITEC, Japan). The solutes used were NaCl, VB_{12}, and myoglobin. In the myoglobin diffusion experiments, a phosphate pH standard equimolal solution (pH = 6.86) was used as the buffer solution. The concentrations of NaCl and vitamin B_{12} were measured using the same methods mentioned earlier, and that of myoglobin was determined spectrophotometrically at $\lambda = 420$ nm on the UV–visible recording spectrophotometer.

The diffusivity of the solute across the microcapsule membrane, D, can also be calculated using a similar equation derived from Fick's first law of diffusion as follows (Chu et al., 2001a)

$$D = \frac{V_m V_s}{V_m + V_s} \cdot \frac{\delta}{A} \cdot \frac{1}{t} \cdot \ln \frac{C_f - C_i}{C_f - C_t} \tag{12}$$

where C_i, C_t, and C_f are the initial, intermediary (at time t), and final concentrations of the solute in the surrounding medium, respectively. The parameters V_m and A are, respectively, the total volume and the total surface area of the microcapsules; δ is the thickness of the membrane of the microcapsule; and V_s is the volume of the surrounding medium.

Results and Discussion

Morphology control of porous membranes with linear-grafted PNIPAM gates

Microcapsule Membranes. Figure 3 shows FE-SEM micrographs of the outer surface and cross-sectional views of the ungrafted and PNIPAM-grafted microcapsules. The ungrafted core-shell polyamide microcapsules are shown to have asymmetrical and porous membrane structures; however, the pore size and the porosity are both smaller than those of the PE flat membrane substrates used in the experiments. Because of their spherical reservoir structures, the microcapsule membranes could be much stronger in restricting the swelling deformation than the PE film substrates. These differences between the two kinds of membrane substrates will result in different solute diffusional properties of the PNIPAM-grafted microcapsule membranes and PE flat ones.

Comparing Figure 3c with Figure 3d, the cross sections of the ungrafted and PNIPAM-grafted microcapsules are seen to have significantly different structures. After grafting PNIPAM onto the inner pore surface of the porous membrane of the microcapsule, the pore size decreased. The porous structure across the cross section of the microcapsule was covered

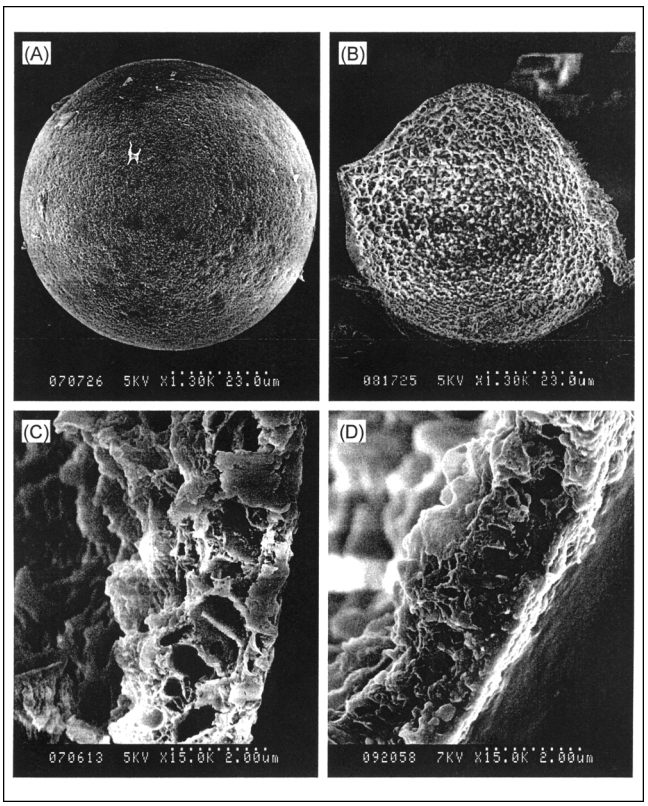

Figure 3. FE-SEM micrographs of microcapsules.

(A) Outer surface; (B) cross section; (C) cross section of an ungrafted microcapsule; (D) cross section of a PNIPAM-grafted microcapsule.

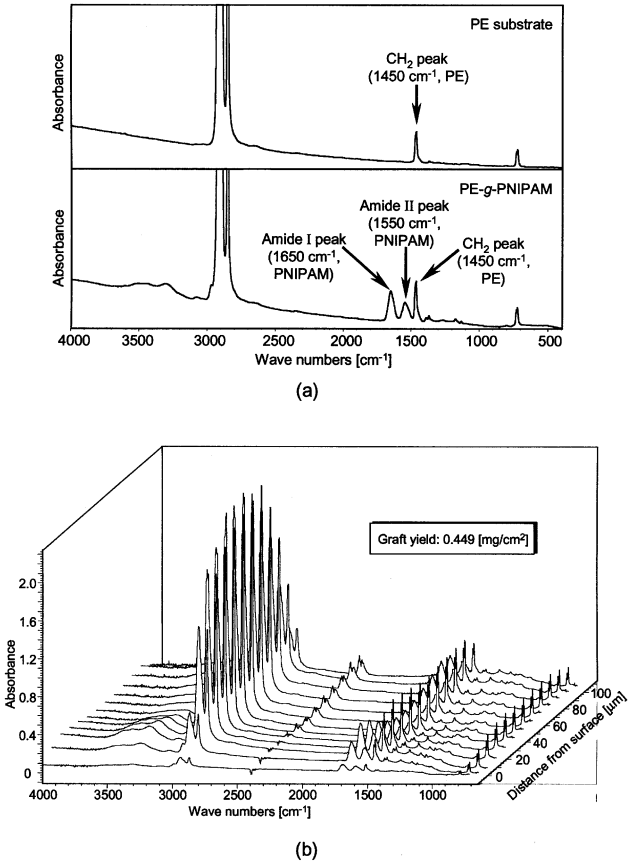

Figure 4. (a) IR spectra of a polyethylene porous membrane before and after the plasma-graft pore-filling polymerization of PNIPAM; (b) a typical IR-mapping spectrum across the thickness of the PE-*g*-PNIPAM membrane.

Degree of grafting = 0.449 mg/cm^2; step size = 10 μm.

homogeneously by the grafted polymer throughout the entire membrane thickness.

PE Flat Membranes. Figure 4a compares the IR spectra of a polyethylene porous membrane before and after the plasma-graft pore-filling polymerization of PNIPAM. The polyethylene substrate exhibits a characteristic methylene peak at 1,450 cm^{-1}. After grafting PNIPAM onto the PE substrate, two characteristic peaks of PNIPAM, the amide I peak (1,650 cm^{-1}) and the amide II peak (1,550 cm^{-1}), appear beside the methylene peak. Therefore, the grafted polymer formation profile could be determined by measuring the height ratio of the PNIPAM characteristic peak to the polyethylene substrate characteristic peak.

Figure 4b shows a typical IR-mapping spectrum across the PE-*g*-PNIPAM membrane thickness. The PNIPAM peaks exist throughout the entire membrane thickness. That implies that the PNIPAM chains were grafted onto the inner surfaces of the pores throughout the entire thickness of the porous membrane. The height ratio of the characteristic PNIPAM peak (amide II peak) to the characteristic polyethylene substrate peak was used to quantitatively characterize the grafting composition of PNIPAM across the membrane thickness. Figure 5a shows a profile of the FT-IR absorbance ratio of the amide II peak to the polyethylene peak in the PNIPAM-grafted membranes. The absorbance ratio was plotted against the distance from the membrane surface. The results show that a roughly homogeneous graft was formed throughout the entire thickness of the membrane, the same as that reported by Choi et al. (2000b). The height ratio of the amide II peak to the characteristic polyethylene peak was found to be directly proportional to the graft yield of PNIPAM, indicating that the grafted polymer formed homogeneously in the pores of the membranes.

Based on the preceding results and discussion, the graft yield of PNIPAM in the membranes could be transformed into the pore-filling ratio as follows

$$F = \frac{Y}{(L \cdot S \cdot \gamma \cdot \rho)/S} \times 100\% \qquad (13)$$

where F is the pore-filling ratio (%), Y is the amount of grafting (mg/cm^2), L is the membrane thickness (cm), S is the membrane surface (cm^2), γ is the porosity of the membrane (dimensionless), and ρ is the density of PNIPAM (g/cm^3). Taking $\rho \cong 1$ g/cm^3, the pore-filling ratio becomes

$$F \cong \frac{Y}{6.90} \times 100\% \qquad (14)$$

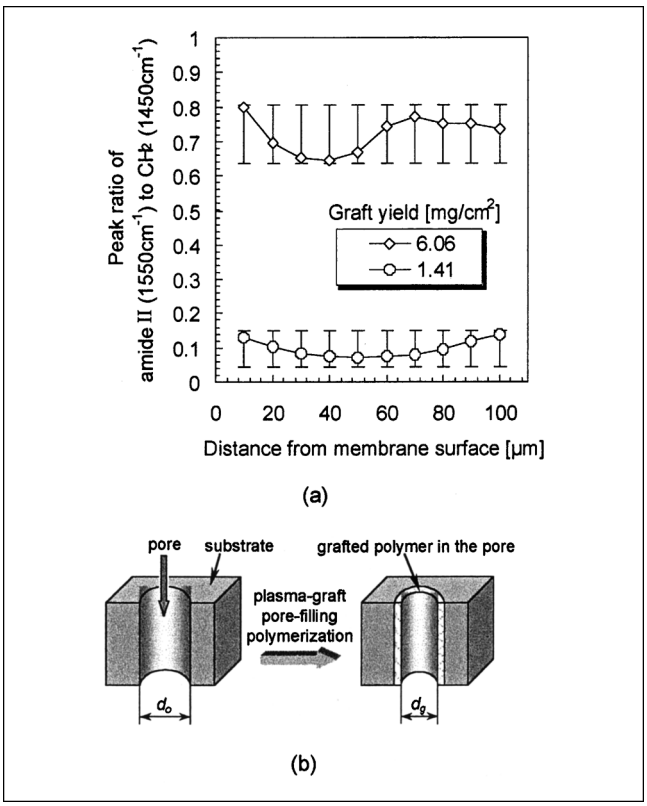

Figure 5. (a) Grafted polymer formation on a cross section of PE-*g*-PNIPAM membrane; (b) membrane pore before and after grafting PNIPAM onto the inner pore surfaces.

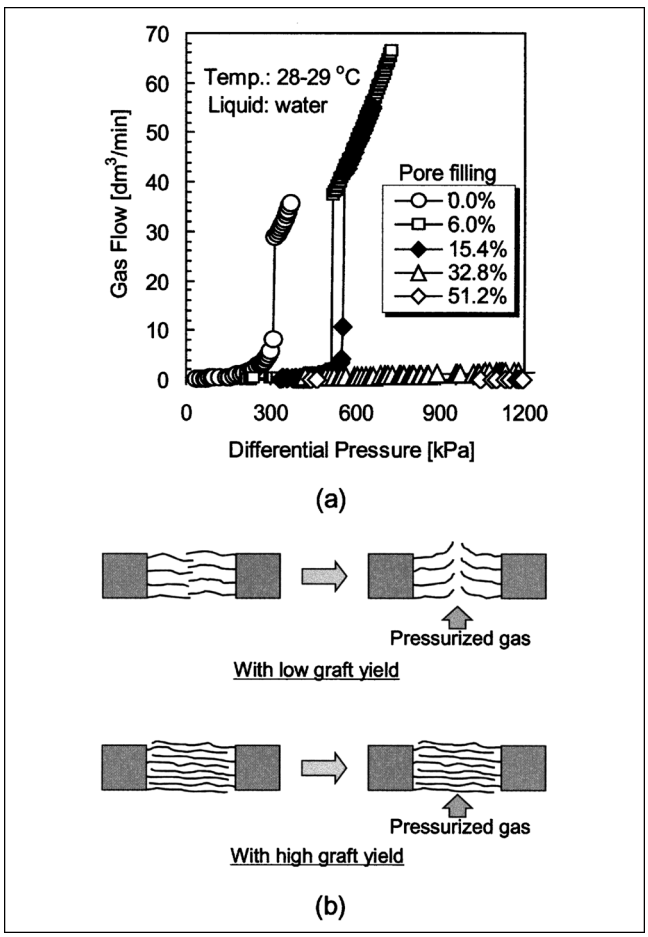

Figure 6. (a) Pore condition of PE-*g*-PNIPAM membranes at temperatures below the LCST of PNIPAM determined by the bubble point method; (b) the pore condition under pressurized gas at temperatures below the LCST of PNIPAM.

Since the grafted polymer can be assumed to be that which formed homogeneously inside the pores, the pore size of the PNIPAM-grafted membrane at temperatures above the LCST can be described as follows

$$d_g = d_o\sqrt{1-F} = d_o\sqrt{1-\varphi} \tag{15}$$

where d_g and d_o are the pore diameters of the membranes after and before the PNIPAM grafting, respectively, as illustrated in Figure 5b.

Table 2 shows a comparison of the calculated to the measured pore sizes of the PE-*g*-PNIPAM membranes, in which the calculation was carried out using Eq. 15, and the measurement was carried out using the mercury intrusion method. The calculated pore sizes agree well with the measured values, indicating again that the PNIPAM chains were homogeneously grafted onto the inner pore surfaces of the membranes throughout the entire membrane thickness.

Table 2. Calculated Pore Sizes of PE-*g*-PNIPAM Membranes Using Eq. 15 vs. Measured Ones Using the Mercury Intrusion Method

Membrane Sample	Filling Ratio [%]	Pore Size [μm]		Relative Error [%]
		Calc.	Meas.	
A	8.1	0.269	0.277	2.89
B	40.0	0.217	0.215	0.93
C	52.0	0.194	0.196	1.02

Figure 6a shows the pore conditions of the PE-*g*-PNIPAM membranes at temperatures below the LCST of PNIPAM determined by the bubble-point method. When the pore-filling ratio was $F \leqq 15.4\%$, the gas flow increased suddenly at the mean flow pore pressures. However, when the pore-filling ratio was $F \geqq 32.8\%$, the gas flows did not increase much, even at high pressures. Since the operational temperatures were lower than the LCST of PNIPAM (about 32°C), and the membranes were in contact with water, the grafted PNIPAM chains in the pores were in the swollen state. However, because the grafted PNIPAM chains have freely mobile ends, the pores could be blown open by the pressurized gas at low PNIPAM graft yields, as illustrated in Figure 6b. On the other hand, for the membranes with high PNIPAM graft yields, the pores could not be blown open by the pressurized gas, be-

cause the grafted PNIPAM chains were probably interwoven with each other, as shown in Figure 6b. The results in Figure 6a show two indications: (1) the PNIPAM chains were grafted tightly on the membrane substrates; and (2) the PNIPAM was grafted homogeneously in the direction of the membrane surface.

In summary, by using the plasma-graft pore-filling polymerization mentioned earlier, PNIPAM was homogeneously grafted onto the PE porous membrane substrates, not only in the direction of the membrane thickness, but also in the direction of the membrane surface.

Effect of membrane morphology on the thermoresponsive transport behavior

Figure 7 shows the effect of the pore-filling ratio of the PE-*g*-PNIPAM membranes on the thermoresponsive diffusional coefficients. The results show that regardless of the molecular size of the solute, the temperature has an opposite effect on the diffusion coefficients of solutes across the membranes with low graft yields as opposed to those with high graft yields. This agrees well with previously reported results (Peng and Cheng, 1998; Chu et al., 2001a). When the graft yield was low, the diffusional coefficients of solutes across the membranes were higher at temperatures above the LCST than those below the LCST, owing to the pores of the membranes being opened/closed as controlled by the shrunken/swollen state changes of the PNIPAM gates. In contrast, when the graft yield was high, the diffusional coefficients were lower at temperatures above the LCST than those below the LCST, owing to the hydrophilic/hydrophobic phase transition of the PNIPAM gates. As the solutes were water soluble, any solute diffusion within the membranes occurred primarily within the water-filled regions in the spaces delin-

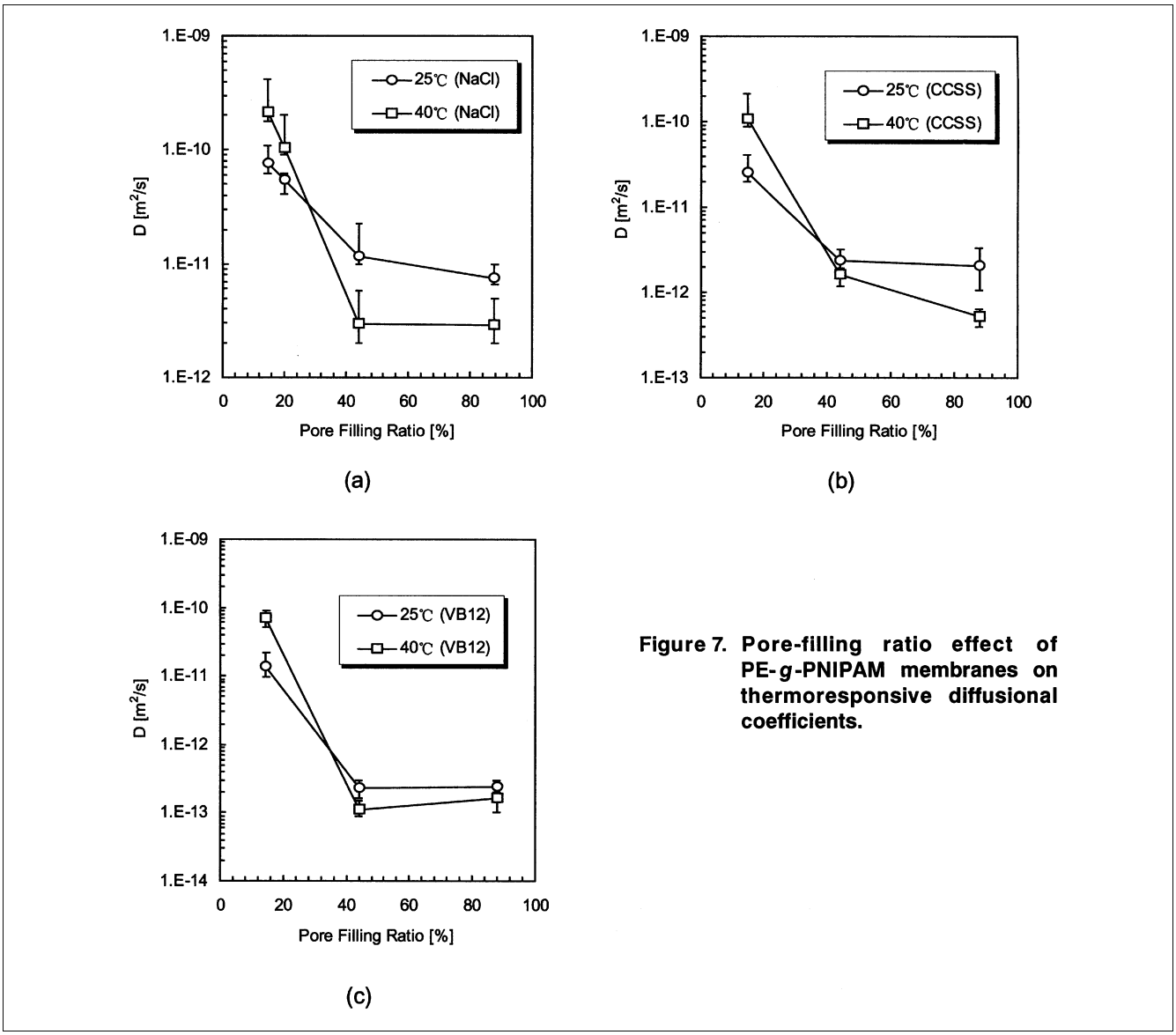

Figure 7. Pore-filling ratio effect of PE-*g*-PNIPAM membranes on thermoresponsive diffusional coefficients.

eated by the PNIPAM chains. It is easier for the solute to find water-filled regions in the membranes with hydrophilic PNIPAM gates rather than in the membranes with hydrophobic PNIPAM gates.

When the diffusional coefficient of the solute across the membrane is higher at temperatures above the LCST than below the LCST, the thermoresponsive membrane can be called a "positive thermoresponse type." In contrast, when

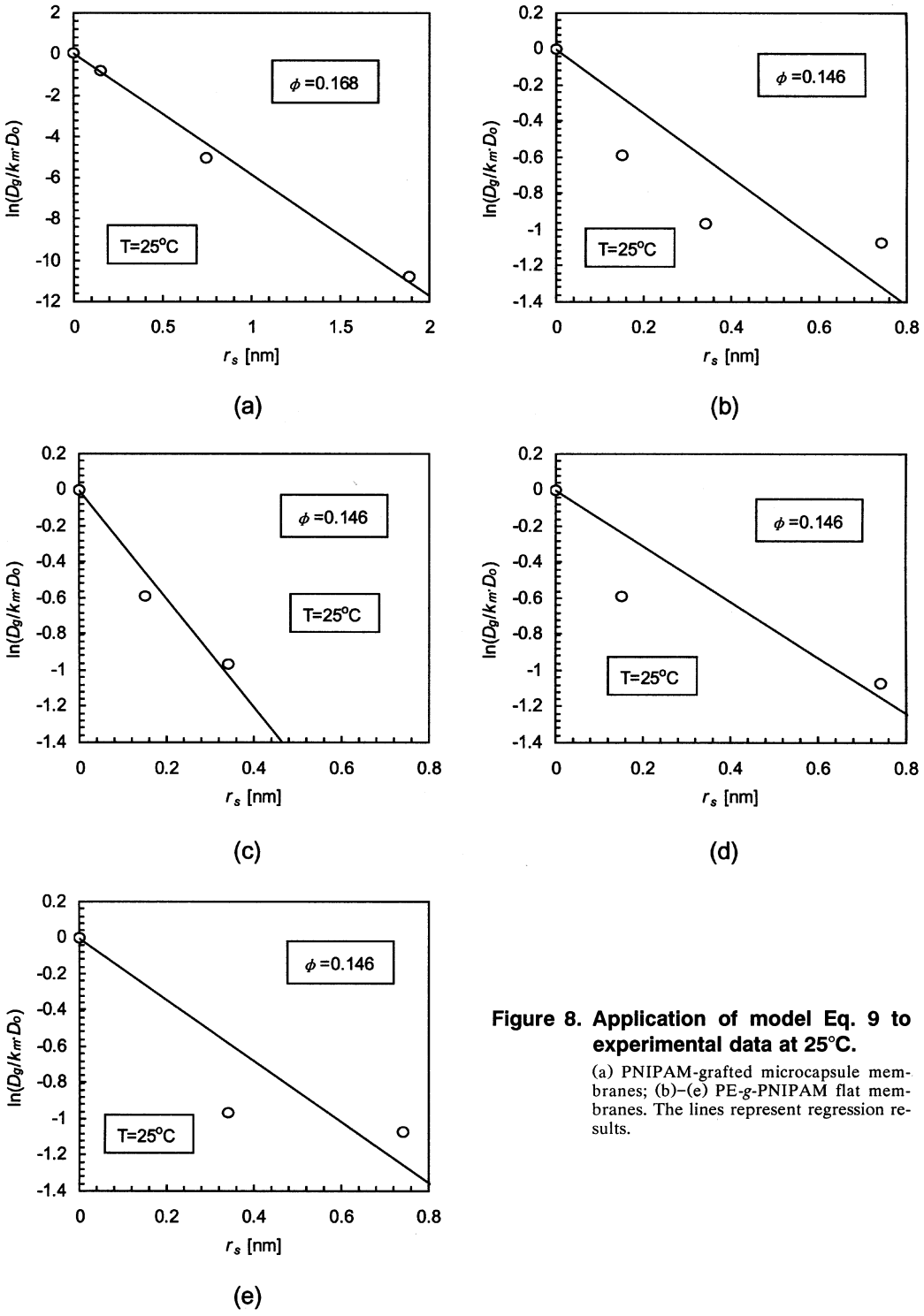

Figure 8. Application of model Eq. 9 to experimental data at 25°C.

(a) PNIPAM-grafted microcapsule membranes; (b)–(e) PE-*g*-PNIPAM flat membranes. The lines represent regression results.

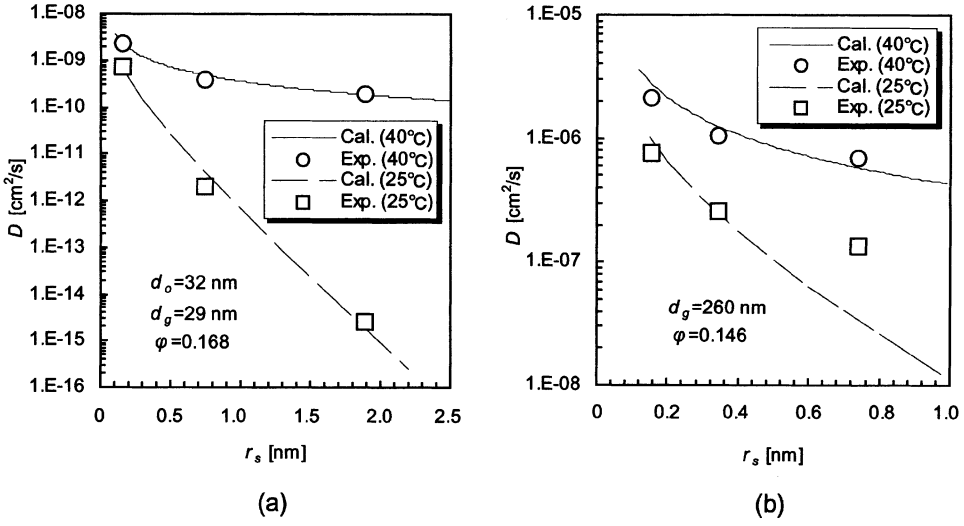

Figure 9. (a) Predicted diffusional coefficients vs. experimental values of the PE-*g*-PNIPAM flat membranes; (b) PNIPAM-grafted microcapsule membranes.

the diffusional coefficient is lower at temperatures above the LCST, the thermoresponsive membrane can be called a "negative thermoresponse type" (Ichikawa and Fukumori, 2000; Chu et al., 2001a). The results in Figure 7 show that, regardless of the molecular size of the solute, the PE-*g*-PNIPAM membranes changed from being positive thermoresponse types to negative thermoresponse types by increasing the pore-filling ratio at around 30%.

Prediction of the thermoresponsive transport behavior with morphological parameters

To estimate the constant k_c in the model (Eq. 9), the model was fit to the experimental data using a linear regression algorithm incorporated into a computer graphing software package (Microsoft Excel). The correlation coefficient (R) was used to carry out the significance test of the linear regression, and the 95% confidence interval (d_{95}) was used to make the interval estimate of the regression constant. The results are illustrated in Figure 8 and Table 3. The results show that the regressions in Figure 8a and Figure 8c were both statistically significant, but the others were not significant enough. This indicates that the model (Eq. 9) is suitable for calculating the diffusional coefficients of the PNIPAM-grafted microcapsule membranes; however, for the PE-*g*-PNIPAM flat membranes, it seems to be only suitable for calculating the diffusional coefficients of those molecules with a relatively small radius.

Figure 9 shows a comparison of the predicted diffusional coefficients with the experimental values of the PNIPAM-grafted microcapsule membranes, and those of the PE-*g*-PNIPAM flat membranes. For the PNIPAM-grafted microcapsule membranes, the model constant $k_c = 2.23$. The predicted diffusional coefficients approximately fit the experimental data at both 40°C and 25°C. This indicates that the PNIPAM was also grafted homogeneously onto the porous membranes of the core-shell microcapsules. For the PE-*g*-PNIPAM flat membranes, the model constant $k_c = 1.27$. At 40°C, the predicted diffusional coefficients fit the experimental data. At 25°C, the predicted diffusivities of NaCl and CCSS also gave a satisfactory fit to the experimental data, but the predicted diffusional coefficient of VB_{12} was much lower than the experimental value. This may have resulted from the weakness of the PE substrate.

Figure 10a shows the swelling ratio of the PE-*g*-PNIPAM membranes at 25°C. The swelling ratio was calculated using the following equation

$$S_1 = \frac{A_w - A_d}{A_d} \times 100\% \tag{16}$$

where S_1 is the swelling ratio of the membrane (%), and A_w and A_d are the areas (cm^2) of water-immersed membrane and dry membrane, respectively.

Table 3. Regression of Application of Model Eq. 9 to Experimental Data at 25°C*

Membranes	Solute	Figure	k_c	$\pm d_{95}$	Q	R
PNIPAM-grafted microcapsule	NaCl, VB_{12}, MYO	8a	2.23	±0.15	0.602	0.9959
PE-*g*-PNIPAM flat	NaCl, CCSS, VB_{12}	8b	0.75	±0.29	0.290	0.7687
PE-*g*-PNIPAM flat	NaCl, CCSS	8c	1.27	±0.18	0.022	0.9766
PE-*g*-PNIPAM flat	NaCl, VB_{12}	8d	0.66	±0.20	0.132	0.8790
PE-*g*-PNIPAM flat	CCSS, VB_{12}	8e	0.72	±0.25	0.182	0.8608

*d_{95}—95% confidence interval for the fitted value of k_c; Q—sum of squares of residuals; and R—Correlation coefficient.

The results in Figure 10a show that the swelling ratio of the PE-*g*-PNIPAM membrane increases with grafting yield, that is, the PE substrates used in the experiments were not strong enough to restrict any conformational change. Therefore, as shown in Figure 10b, at temperatures below the LCST of PNIPAM, the grafted PNIPAM chains in the pores were in the swollen state, and, therefore, the substrates were subjected to a pressure arising from the swelling of the PNIPAM gates. As a result, weak substrates may be constricted or deformed. On the other hand, strong substrates would be expected not to have any deformation. Consequently, for solute diffusion, the dimensions of the water-filled regions delineated by the PNIPAM chains are expected to be larger in the membranes prepared with weak substrates than those prepared with strong substrates, that is, it was easier for the solutes to pass through the membranes with weak substrates. In other words, if PNIPAM-grafted membranes were prepared with strong substrates, the predicted diffusional coefficients of solutes with larger molecular sizes would also be expected to fit the experimental data at temperatures below the LCST.

For the PNIPAM-grafted membranes prepared with weak substrates, the variable that describes the pore-filling ratio or the volume fraction of polymer in the gel in Eq. 9 should be modified owing to this substrate swelling effect. Introducing the term φ_m to describe the modified pore-filling ratio that reflects the swelling effect of the membrane substrate, and taking the substrate swelling as a linear movement in all three dimensions, then from Eqs. 13, 15 and 16, the modified φ_m term can be calculated as follows

$$\varphi_m = \frac{\gamma \cdot \varphi}{\left(\frac{S_1}{100}+1\right)^{3/2} \cdot \left[1-\left(\frac{S_1}{100}+1\right)^{-3/2}(1-\gamma)\right]} \quad (17)$$

where S_1 is the swelling ratio of membrane (%) as defined in Eq. 16, γ is the porosity of the membrane (dimensionless) as used in Eq. 13, and φ is the volume fraction of polymer in the gel or the pore-filling ratio that disregards any swelling effect.

The predicted results obtained by using the modified φ_m term in Eq. 9 are shown in Figure 11. Just as expected, by taking the swelling effect into account, the calculated diffusional coefficients at 25°C also fit well with the experimental data of the PE-*g*-PNIPAM flat membranes.

From the preceding results and discussion, it is confirmed that the phenomenological models (Eqs. 7 and 9) are suitable for describing the thermoresponsive diffusional behavior of solutes across the PNIPAM-grafted membranes.

Figure 12 shows the predicted results of the effects of membrane pore size, pore-filling ratio, and the solute molecular size on the diffusional coefficients of solutes across the PNIPAM-grafted membranes (let $k_m = 0.0001$ arbitrarily), in which the model constant k_c is selected as 1.1 arbitrarily. At temperatures above the LCST of PNIPAM, the diffusional coefficient of a solute is principally dependent on the membrane pore size, the pore-size distribution, and the molecular size of the solute. Generally, the diffusional coefficient at temperatures above the LCST increases with the increasing mean diameter of the membrane pores, and decreases with the increasing molecular size of the solute.

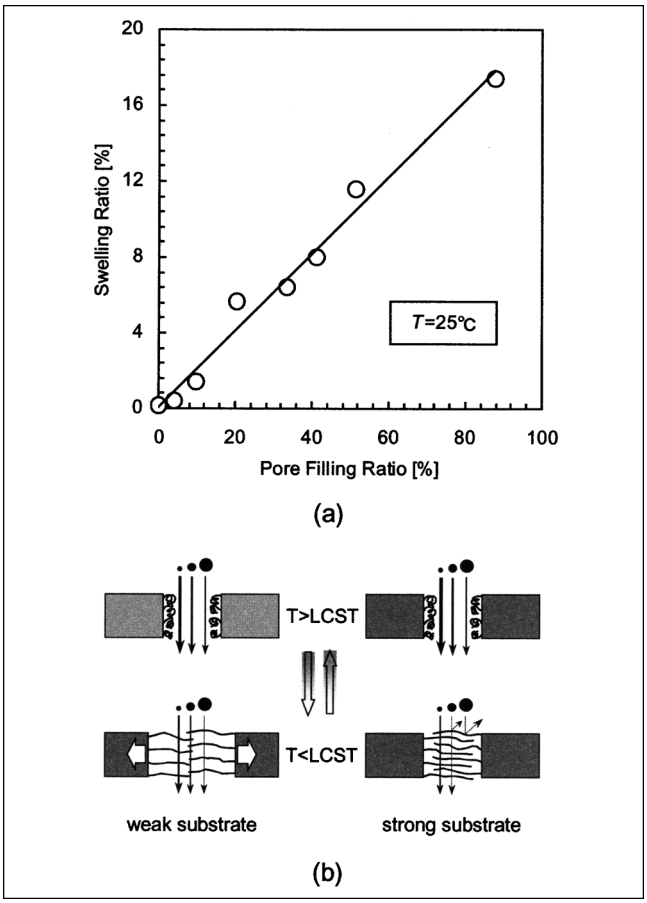

Figure 10. (a) Swelling ratio of membranes; (b)diffusional permeations of solutes across PNIPAM-grafted membranes for weak and strong substrates.

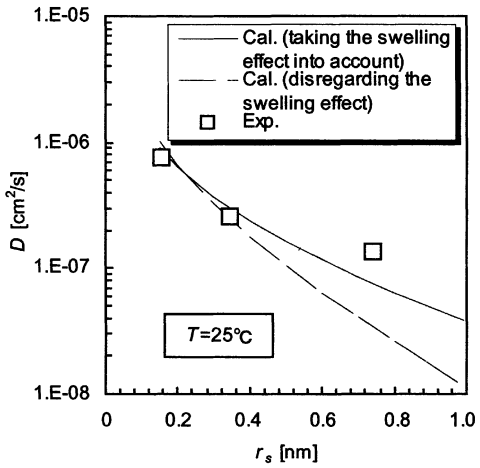

Figure 11. Prediction of diffusional coefficients of PE-*g*-PNIPAM flat membranes considering the swelling effect of membranes.

At temperatures below the LCST of PNIPAM, the diffusional coefficient of a solute is principally dependent on the pore-filling ratio of the PNIPAM-grafted membrane and the molecular size of the solute. Generally, the diffusional coefficient at temperatures below the LCST decreases with increasing pore-filling ratio, and decreases with increasing molecular size of the solute. When the molecular size of the solute is small, the diffusional coefficient decreases slowly with the increasing pore-filling ratio. However, when the molecular size of a solute is large, the diffusional coefficient decreases rapidly with the increasing pore-filling ratio.

Conclusions

In this study, both thermoresponsive flat membranes and core-shell microcapsule membranes with a porous membrane substrate and grafted PNIPAM gates were successfully prepared using a plasma-graft pore-filling polymerization method. PNIPAM was proven to be homogeneously grafted onto the PE porous membrane substrates, not only in the direction of the membrane thickness, but also in the direction of the membrane surface.

Regardless of the molecular size of the solute, temperature had an opposite effect on the diffusion coefficients of the solutes across the PNIPAM-grafted membranes with low graft yields as opposed to those with high graft yields. When the pore-filling ratio was below ~30%, the diffusional coefficients of the solutes across the PNIPAM-grafted membranes were higher at temperatures above the LCST than those below the LCST. In contrast, when the pore-filling ratio was higher than ~30%, the diffusional coefficients were lower at temperatures above the LCST than those below the LCST.

Phenomenological models for predicting the diffusion coefficient of a solute across PNIPAM-grafted membranes at temperatures both above and below the LCST were developed in this study. The predicted diffusional coefficients of solutes across both PNIPAM-grafted flat membranes and PNIPAM-grafted microcapsule membranes were shown to fit with experimental values.

To obtain ideal results for diffusional thermoresponsive controlled-release through PNIPAM-grafted membranes, those substrates strong enough to prevent any conformation changing should be used in the preparation of the thermoresponsive membranes rather than weak substrates.

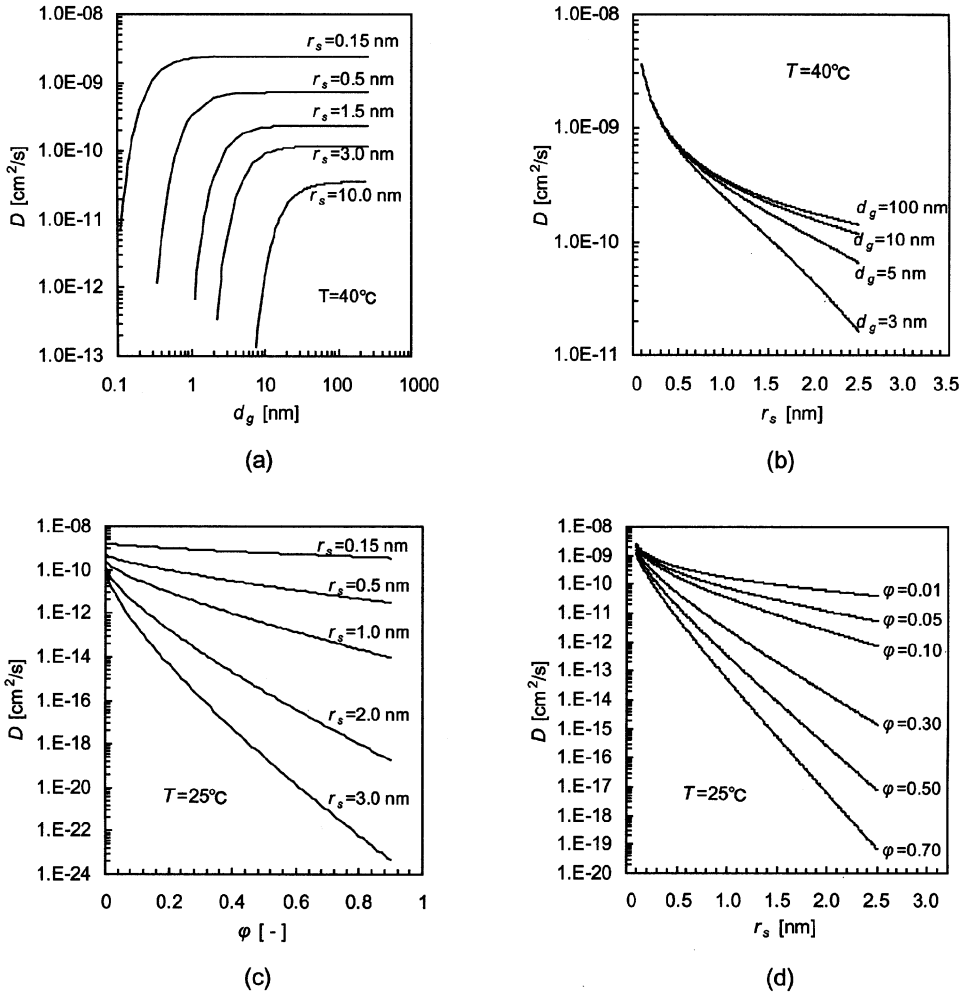

Figure 12. Effect of membrane morphological parameters and solute molecular size on diffusional coefficients of solutes across PNI-PAM-grafted membranes.

Acknowledgments

The authors thank Messrs. Sang-Hoon Park and Takashi Sugawara of the Department of Chemical System Engineering at the University of Tokyo for their advice and help in carrying out the experimental work, and the Kohjin Co., Ltd., Japan, for kindly supplying the *N*-isopropylacrylamide.

Literature Cited

Amsden, B., "Solute Diffusion within Hydrogels. Mechanisms and Models," *Macromolecules,* **31,** 8382 (1998a).

Amsden, B., "Solute Diffusion in Hydrogels. An Examination of the Retardation Effect," *Poly. Gels Networks,* **6**, 13 (1998b).

Amsden, B., "An Obstruction-Scaling Model for Diffusion in Homogeneous Hydrogels," *Macromolecules,* **32,** 874 (1999).

Bhaskar, R. K., R. V. Sparer, and K. J. Himmelstein, "Effect of an Applied Electric Field on Liquid Crystalline Membranes: Control of Permeability," *J. Memb. Sci.,* **24,** 83 (1985).

Cartier, S., T. A. Horbett, and B. D. Ratner, "Glucose-Sensitive Membrane Coated Porous Filters for Control of Hydraulic Permeability and Insulin Delivery from a Pressurized Reservoir," *J. Memb. Sci.,* **106,** 17 (1995).

Chen, G., Y. Ito, and Y. Imanishi, "Regulation of Growth and Adhesion of Cultured Cells by Insulin Conjugated with Thermoresponsive Polymers," *Biotechnol. Bioeng.,* **53,** 339 (1997).

Choi, Y.-J., T. Yamaguchi, and S. Nakao, "A Novel Separation System Using Porous Thermosensitive Membranes," *Ind. Eng. Chem. Res.,* **39,** 2491 (2000a).

Choi, Y.-J., T. Yamaguchi, and S. Nakao, "Morphology Control of Thermosensitive Membranes and Fundamental Investigation of Its Protein Purification," *Kagaku-Kogaku Ronbunshu,* **26,** 849 (2000b).

Chu, L.-Y., S.-H. Park, T. Yamaguchi, and S. Nakao, "Preparation of Thermo-Responsive Core-Shell Microcapsules with a Porous Membrane and Poly(*N*-Isopropylacrylamide) Gates," *J. Memb. Sci.,* **192,** 27 (2001a).

Chu, L. Y., S. H. Park, T. Yamaguchi, and S. Nakao, "Thermo-Responsive Core-Shell Microcapsules with a Porous Membrane and PNIPAM Gates," *Jpn. Fiber Preprints,* **56**, 76 (2001b).

Chu, L. Y., S. H. Park, T. Yamaguchi, and S. Nakao, "Preparation of Micron-Sized Monodispersed Thermo-Responsive Core-Shell Microcapsules," *Langmuir,* **18,** 1856 (2002a).

Chu L.Y., T. Yamaguchi, and S. Nakao, "A Molecular-Recognition Microcapsule for Environmental Stimuli-Responsive Controlled-Release," *Adv. Mater.,* **14**, 386 (2002b).

Chung, D.-J., Y. Ito, and Y. Imanishi, "Preparation of Porous Membranes Grafted with Poly(spiropyran-containing methacrylate) and Photocontrol of Permeability," *J. Appl. Poly. Sci.*, **51**, 2027 (1994).

Cukier, R. I., "Diffusion of Brownian Spheres in Semidilute Polymer Solutions," *Macromolecules,* **17,** 252 (1984).

Hautojarvi, J., K. Kontturi, J. H. Nasman, B. L. Svarfvar, P. Viinikka, and M. Vuoristo, "Characterization of Graft-Modified Porous Polymer Membranes," *Ind. Eng. Chem. Res.,* **35,** 450 (1996).

Ichikawa, H., and Y. Fukumori, "A Novel Positively Thermosensitive Controlled Release Microcapsule with Membrane of Nano-Sized Poly(*N*-isopropylacrylamide) Gel Dispersed in Ethylcellulose Matrix," *J. Controlled Release,* **63,** 107 (2000).

Islam, M. A., A. Dimov, and A. L. Malinova, "Environment-Sensitive Properties of Polymethacrylic Acid-Grafted Polyethylene Membranes," *J. Memb. Sci.,* **66,** 69 (1992).

Israels, R., D. Gersappe, M. Fasolka, V. A. Roberts, and A .C. Balazs, "pH-Controlled Gating in Polymer Brushes," *Macromolecules,* **27,** 6679 (1994).

Ito, Y., M. Casolaro, K. Kono, and Y. Imanishi, "An Insulin-Releasing System that Is Responsive to Glucose," *J. Controlled Release,* **10,** 195 (1989).

Ito, Y., M. Inaba, D.-J. Chung, and Y. Imanishi, "Control of Water Permeation by pH and Ionic Strength Through a Porous Membrane Having Poly(carboxylic Acid) Surface-Grafted," *Macromolecules,* **25,** 7313 (1992).

Ito, Y., S. Kotera, M. Inaba, K. Kono, and Y. Imanishi, "Control of Pore Size of Polycarbonate Membrane with Straight Pores by Poly(acrylic Acid) Grafts," *Polymer,* **31,** 2157 (1990).

Ito, Y., S. Nishi, Y. S. Park, and Y. Imanishi, "Oxidoreduction-Sensitive Control of Water Permeation Through a Polymer Brushes-Grafted Porous Membrane," *Macromolecules,* **30,** 5856 (1997a).

Ito, Y., Y. Ochiai, Y. S. Park, and Y. Imanishi, "pH-Sensitive Gating by Conformational Change of a Polypeptide Brush Grafted onto a Porous Polymer Membrane," *J. Amer. Chem. Soc.,* **119,** 1619 (1997b).

Ito, Y., Y. S. Park, and Y. Imanishi, "Visualization of Critical pH-Controlled Gating of a Porous Membrane Grafted with Polyelectrolyte Brushes," *J. Amer. Chem. Soc.,* **119,** 2739 (1997c).

Iwata, H., and T. Matsuda, "Preparation and Properties of Novel Environment-Sensitive Membranes Prepared by Graft Polymerization onto a Porous Membrane," *J. Memb. Sci.,* **38,** 185 (1988).

Iwata, H., M. Oodate, Y. Uyama, H. Amemiya, and Y. Ikada, "Preparation of Temperature-Sensitive Membranes by Graft Polymerization onto a Porous Membrane," *J. Memb. Sci.,* **55,** 119 (1991).

Johansson, L., C. Elvingston, and J. E. Lofroth, "Diffusion and Interaction in Gels and Solutions: 3. Theoretical Results on the Obstruction Effect," *Macromolecules,* **24,** 6024 (1991).

Kim, J. T., and J. L. Anderson, "Hindered Transport Through Micropores with Adsorbed Polyelectrolytes," *J. Memb. Sci.,* **47,** 163 (1989).

Kubota, H., N. Nagaoka, R. Katakai, M. Yoshida, H. Omichi, and Y. Hata, "Temperature-Responsive Characteristics of *N*-Isopropylacrylamide-Grafted Polymer Films Prepared by Photografting," *J. Appl. Poly. Sci.,* **51,** 925 (1994).

Lee, Y. M., S. Y. Ihm, J. K. Shim, J. H. Kim, C. S. Cho, and Y. K. Sung, "Preparation of Surface-Modified Stimuli-Responsive Polymeric Membranes by Plasma and Ultraviolet Grafting Methods and Their Riboflavin Permeation," *Polymer,* **36,** 81 (1995).

Lee, Y. M., and J. K. Shim, "Plasma Surface Graft of Acrylic Acid onto a Porous Poly(vinylidene Fluoride) Membrane and Its Riboflavin Permeation," *J. Appl. Poly. Sci.,* **61,** 1245 (1996).

Ly, Y., and Y.-L. Cheng, "Electrically-Modulated Variable Permeability Liquid Crystalline Polymeric Membrane," *J. Memb. Sci.,* **77,** 99 (1993).

Mika, A. M., R. F. Childs, J. M. Dickson, B. E. McCarry, and D. R. Gagnon, "A New Class of Polyelectrolyte-Filled Microfiltration Membranes with Environmentally Controlled Porosity," *J. Memb. Sci.,* **108,** 37 (1995).

Ogston, A. G., "The Spaces in a Uniform Random Suspension of Fibers," *Trans. Faraday Soc.,* **54,** 1754 (1958).

Okahata, Y., H.-J. Lim, G. Nakamura, and S. Hachiya, "A Large Nylon Capsule Coated with a Synthetic Bilayer Membrane. Permeability Control of NaCl by Phase Transition of the Dialkylammonium Bilayer Coating," *J. Amer. Chem. Soc.,* **105,** 4855 (1983).

Okahata, Y., H. Noguchi, and T. Seki, "Thermoselective Permeation from a Polymer-Grafted Capsule Membrane," *Macromolecules,* **19,** 493 (1986).

Okahata, Y., H. Noguchi, and T. Seki, "Functional Capsule Membranes: 26. Permeability Control of Polymer-Grafted Capsule Membranes Responding to Ambient pH Changes," *Macromolecules,* **20,** 15 (1987).

Osada, Y., K. Honda, and M. Ohta, "Control of Water Permeability by Mechanochemical Contraction of Poly(methacrylic Acid)-Grafted Membranes," *J. Memb. Sci.,* **27,** 327 (1986).

Peng, T., and Y.-L. Cheng, "Temperature-Responsive Permeability of Porous PNIPAAm-*g*-PE Membranes," *J. Appl. Poly. Sci.,* **70,** 2133 (1998).

Peng, T., and Y.-L. Cheng, "pH-Responsive Permeability of PE-*g*-PMAA Membranes," *J. Appl. Poly. Sci.,* **76,** 778 (2000).

Shim, J. K., Y. B. Lee, and Y. M. Lee, "pH-Dependent Permeation Through Polysulfone Ultrafiltration Membranes Prepared by Ultraviolet Polymerization Technique," *J. Appl. Poly. Sci.,* **74,** 75 (1999).

Ulbricht, M., "Photograft-Polymer-Modified Microporous Membranes with Environment-Sensitive Permeabilities," *React. Funct. Polym*, **31,** 165 (1996).

Yamaguchi, T., T. Ito, T. Sato, T. Shinbo, and S. Nakao, "Development of a Fast Response Molecular Recognition Ion Gating Membrane," *J. Amer. Chem. Soc.,* **121,** 4078 (1999).

Yamaguchi, T., S. Nakao, and S. Kimura, "Plasma-Graft Filling Polymerization: Preparation of a New Type of Pervaporation

Membrane for Organic Liquid Mixtures," *Macromolecules,* **24,** 5522 (1991).
Yamaguchi, T., S. Nakao, and S. Kimura, "Evidence and Mechanisms of Filling Polymerization by Plasma-Induced Graft Polymerization," *J. Poly. Sci., Poly. Chem. Ed.,* **34,** 1203 (1996).
Yasuda, H., A. Peterlin, C. K. Colton, K. A. Smith, and E. W. Merrill, "Permeability of Solutes Through Hydrated Polymer Membranes: Part III. Theroretical Background for the Selectivity of Dialysis Membranes," *Makromol. Chem.,* **126,** 177 (1969).
Yoshida, Y., K. Uchida, Y. Kaneko, K. Sakai, A. Kikuchi, Y. Sakurai, and T. Okano, "Comb-Type Grafted Hydrogels with Rapid De-Swelling Responsive to Temperature Changes," *Nature,* **374,** 240 (1995).

Manuscript received Feb. 4, 2002, and revision received Sept. 12, 2002.